Structural Analysis of Historical Constructions, New Delhi 2006
P.B. Lourenço, P. Roca, C. Modena, S. Agrawal (Eds.)

Retrofitting of Masonry Arch Bridges with FRP

G. Buffarini
ENEA Casaccia Research Centre, Rome, Italy

P. Clemente
ENEA Casaccia Research Centre, Rome, Italy

G. de Felice
Dept. of Structures, University Roma Tre, Italy

ABSTRACT: A procedure for limit analysis of masonry arch bridges reinforced with FRP is proposed which takes into account the failure modes that may develop in reinforced cross sections and can be used as a tool for strengthening of bridges under travelling loads, under condition that failure is still controlled by the hinge collapse mechanism.

1 INTRODUCTION

Masonry arches represent one of the most interesting topics in the field of structural analysis of historic and monumental structures. One of the reason of this interest, which date back to the pioneeristic studies of the eighteen and nineteen centuries, lies in the assessment of effective load carrying capacity of structures which are still in use; think for instance to existing railway arch bridges, which have to comply with current revisions and updating of loading conditions.

A suitable interpretation of the limit behaviour of masonry arches is given by the mechanism model, in which failure occurs only when a sufficient number of "hinges" forms to turn the structure into a mechanism.

Among the different techniques proposed for strengthening masonry arches, the use of fibre reinforced polymers (FRP) appears one of the most promising methods, and guidelines for FRP strengthening of masonry structures is currently under public revision. When the reinforcement is applied, either at the intrados or at the extrados, the behaviour of the arch changes significantly. In fact, the reinforcement acts as a constraint for a class of mechanism by increasing, at the same time, the compression stress in the cross-section. Therefore, masonry compression strength can no longer be considered as infinite and crushing in compression must be checked. In the presence of reinforcement, the trust line is allowed to go out of the cross section and can assume a high slope with respect to the centre line of the arch; as a result sliding between voussoirs may occur and must be checked as well. Besides, ripping or debonding of FRP, together with tensile failure of FRP strips must be checked too.

The application of FRP may strongly increase the load carrying capacity of masonry arches; however, the appraisal of the new aforementioned collapse mechanism, which may occur with limited ductility, is one of the main drawbacks of this strengthening technique.

The purpose of this paper is to present a methodology for the design of FRP reinforcement of masonry arch bridges under travelling loads, which responds to the demand of increasing the load carrying capacity of the bridge, without the appraisal of new mechanisms. It is a sort of capacity design in which the extension of the reinforcement to be applied at the extrados, or at the intrados, of the vault is obtained under condition that the capacity is still controlled by the hinge collapse mechanism.

After a brief review of the classical approach of limit analysis of masonry arch bridges under travelling loads (section 2), and a recall of limit states for FRP reinforced sections (section 3), the increase in load carrying capacity due to application of FRP, of variable length, at the intra-

dos or at the extrados of the arch is analysed for single-span arch bridges with fixed abutments and for multi-span arch bridges, taking into account the collapse of the piers.

2 STRUCTURAL BEHAVIOUR OF MASONRY ARCH BRIDGES

The modern study of masonry arches dates back to the well-known papers in which Heyman (1966 and 1969) supplied a comprehensive state-of-the-art knowledge on the subject, including theoretical and experimental results of the last three centuries. The results of these studies may be summarized as follows: collapse must be viewed as a geometrical problem rather than as a problem of strength of materials; failure of the arch is not related to crushing of masonry, but only to its shape.

2.1 The collapse of masonry arch bridges

The application of plastic theory to masonry is based on the following three hypotheses on material behaviour: a) joints between voussoirs have no tensile strength, due to the absence or to the weakness of mortar between masonry units; b) compression strength is assumed to be infinite, since the stresses are low enough to avoid crushing of the material; c) sliding failure cannot occur, since friction between voussoirs is high enough to avoid sliding.

Referring to a vault with rectangular cross-section of width *b* and height *t*, the strength condition in the plane (N_d, M_d) of normal force and bending moment on the cross section due to external load, is given by:

$$\left|M_d\right| \leq N_d \; t/2 \tag{1}$$

Cross section failure corresponds to a state of stress in which the resultant axial force N_d lies at the extrados or at the intrados of the cross-section; the eccentricity *e* is given by:

$$e = M_d / N_d = \pm t/2 \tag{2}$$

In this condition, a hinge forms at the free edge; failure of the vault occurs when sufficient number of hinges form to turn the structure into a mechanism (Fig. 1).

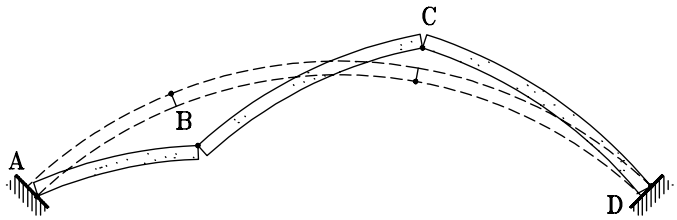

Figure 1 : Collapse mechanism of a masonry arch

In other words, the arch will stand until a line of thrust in equilibrium under external loading exists that lie wholly within the arch profile. Let us point out that, according to the safe theorem, the line of thrust in equilibrium need not to be the actual line of thrust, which is unknown, since no assumptions have been made on material constitutive behaviour. The actual stress in the cross section is also unknown.

2.2 Limit analysis under travelling loads

Referring to Fig. 2, consider an incoming travelling load *q* uniformly distributed from the left springing of the bridge to a generic section denoted by z_L; the bearing capacity of the bridge, expressed by the load factor λ, can be evaluated according to limit analysis kinematic approach as follows. Denoting by $\eta(z)$ the vertical component of a kinematic admissible linearized displacement, using the principle of virtual work to express equilibrium in a dual form, it appears that a necessary condition for the bridge to carry live load λq is given by:

$$L_g(\eta) + \lambda\, L_q(\eta) \le 0 \qquad \text{whatever} \quad \eta \tag{3}$$

where the two terms in eq. (3) represent the virtual works, in the failure mechanism η, of dead load and travelling load respectively, while, according to previous assumptions, there is no internal work:

$$L_g(\eta) = \int_0^L (g_0 + g_1)\eta \; dz, \qquad L_q(\eta) = \int_0^{z_L} q \; \eta \; dz \; , \tag{4}$$

g_0 and g_1 being the self-weight per unit length, of masonry arch and backfill respectively.

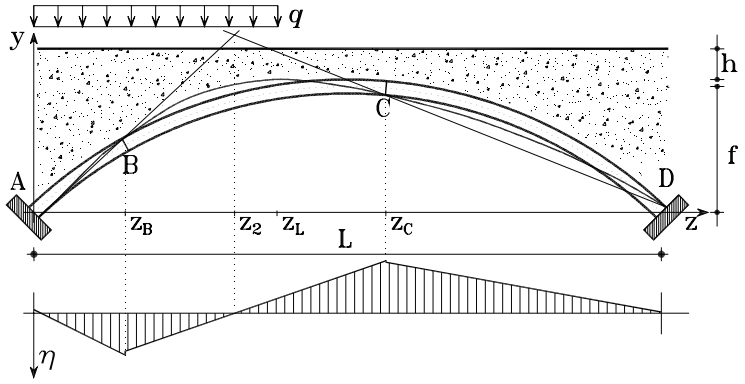

Figure 2 : Arch model

The effective collapse mechanism and the corresponding live load factor can be found searching for the minimum load factor $\lambda = -L_g / L_q$ that comply with eq. (3). An iteration procedure can be used to this purpose based on the exploration of all possible hinges location. This can be started giving a first mechanism and the corresponding diagram of vertical displacement. The value λ given by eq. (3) is the collapse load factor only if the funicular polygon passing through the hypothesized hinges is elsewhere within the masonry; if it is not, in the next step we must move the hinges to the cross-sections having the maximum distances between the funicular polygon and the arch profile. The procedure ends when a funicular polygon is reached that lies entirely within the arch profile (see Clemente et al. 1995 for details).

3 FAILURE MODES OF FRP REINFORCED CROSS-SECTION

For arches reinforced with FRP, the two hypothesis b) and c) given in section 2.1, are no longer valid, since crushing and sliding may occur due to the increase in bending capacity provided by the reinforcement.

In this section, the limit state conditions of FRP reinforced cross-section, which will be used in subsequent numerical investigations, are briefly reminded. For more details see Triantafillou (1998), Faccio et al. (2000), Foraboschi (2001, 2004).

Let us assume, as suggested by Triantafillou (1998), Faccio et al. (2000), that FRP strips may be considered as non-active until the line of thrust lies into the cross-section. So, if the eccentricity $e \le t/2$, then the section behaves like the non-strengthened section and only compression stresses are needed for the equilibrium. Only if $e > t/2$, the FRP contribution is required for the equilibrium at the edge where the crack forms. In this case, the tensile force T that develops in FRP strips is balanced by an increase in the compressive force C in the cross section at the edge opposite to the reinforcement:

$$C = N_d + T \tag{5}$$

3.1 Crushing of masonry in compression

According to experimental evidences (Foraboschi, 2004), the resulting compression stress C can be assumed to be uniformly distributed over a thickness $t/3$ (Fig. 3). In order to avoid crushing of masonry that may occur in reinforced cross-sections (but not in non-reinforced ones), the compression C should not exceed the limit compression C_u given by

$$C_u = f_m \tilde{b} t/3 \tag{6}$$

where f_m is the strength of masonry in compression, $\tilde{b}$ is the width of the cross section that absorbs the increase in compression, which depends on the position of reinforcement (number, width and relative distance of strips), on the masonry work and on the level of axial forces. In the following $\tilde{b}$ has been assumed to be equal to the total width $\tilde{b}$ of the arch, which means that the FRP strips are deployed over the whole arch depth. The ultimate bending moment after which crushing takes place is therefore:

$$M_u = 5/6 \cdot C_u - 1/2 \cdot N_d t \tag{7}$$

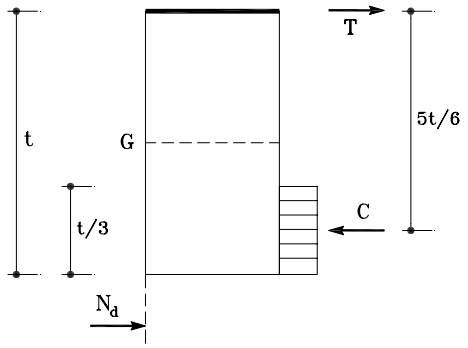

Figure 3 : Equilibrium of the reinforced cross-section

3.2 Shear failure

The shear forces is usually very low in non reinforced arches, it can become high in reinforced arches when the line of thrust lies outside of the cross section and assume a high slope with respect to the arch profile. It is worth noting that if the resultant is external of the cross section, then the compression force C increases according to (5) and shear resistance increases too. To avoid shear failure, the shear V_d due to external load should not exceed the ultimate shear V_u given by:

$$V_u = \mu C \tag{8}$$

where μ is the friction coefficient of masonry.

3.3 Debonding and FRP tensile failure

Collapse of FRP may occur either to debonding of strips or to tensile failure of reinforcement. As a result of the curvature of the arch, when the FRP strip is in tension not only shear stress, but also normal stress $\sigma_\perp$, develops at the interface between strip and masonry:

$$\sigma_\perp = T/(n\, w\, R) \tag{9}$$

where n is the number of reinforcement strips, w their width and R the radius of curvature of the arch. If the reinforcement is applied at the intrados of the arch bridge, $\sigma_\perp$ is a traction and therefore debonding may occur. It can be shown (Foraboschi 2004) that if the reinforcement is properly applied, the cracks develop in masonry rather than in epoxy matrix, with the ripping of a thin layer of brickwork; denoting by f_{mt} the tensile strength of brickwork, the ultimate traction in FRP strips to prevent ripping is given by:

$$T_{bu} = n\, f_{mt} w\, R \tag{10}$$

and the corresponding ultimate bending moment is:

$$M_{bu} = \frac{5}{6} T_{bu}\, t + \frac{1}{3} N_d\, t \tag{11}$$

Finally, denoting by f_t the tensile resistance of reinforcement per unit width of strip, then the limit traction in FRP strips to prevent tensile failure is given by:

$$T_{tu} = n\, w\, f_t \tag{12}$$

The corresponding bending moment is:

$$Mt_{tu} = \frac{5}{6} T_{tu}\, t + \frac{1}{3} N_d\, t \tag{13}$$

4 LIMIT ANALYSIS OF REINFORCED MASONRY ARCH BRIDGES AND APPLICATIONS

The application of FRP strips at the intrados or at the extrados increase the strength of the arch: in fact, some collapse mechanisms are restraint, since opening of the joints on the reinforcement side is not permitted, and the line of trust is allowed to lie out of the arch profile at the opposite edge of reinforcement. However, as a consequence, the local failure modes described in the previous paragraph become possible and have to be checked.

The same procedure used for limit analysis of non reinforced masonry arches can be applied to reinforced arches but, in this case, the set of failure mechanisms to be investigated according to the kinematic approach, is only a subset of the previous one. Therefore, the search for the minimum load factor $\lambda = -L_g / L_q$ that comply with eq. (3), in the subset of mechanisms allowed by the reinforcement, will give rise to a collapse load multiplier not lower than that of non-reinforced arch.

Once the effective collapse mechanism is found, the corresponding line of trust can be traced (Fig. 4), and the conditions on local strength can be checked according to the expressions available in the literature as recalled in section 3.

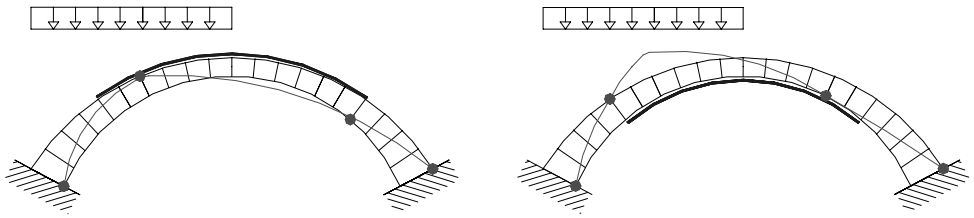

Figure 4 : Hinge locations and thrust line for FRP at the extrados and at the intrados

If the conditions on local strength are not fulfilled, then the design of reinforcement has to be modified, either by reducing the extension of reinforcement or by increasing the number *n* of strips. Once the conditions on local strength are satisfied with the desired safety factor, this ensure that the load factor is the one obtained and failure will develop with the classical hinge mechanism. The reinforcement designed according to this procedure ensures ductility similar to that of non reinforced arch together with an increase in load carrying capacity.

As an application to the procedure previously described, consider the arch bridge having rise-to-span ratio $f/L = 0.20$ and depth-to-span ratio $t/L = 0.03$, subject to the dead load g_0 and g_1, and to the normalized travelling incoming load

$$q = \frac{1}{L} \int_0^L (g_0 + g_1)\, dz \tag{14}$$

The weight per unit volume of the arch is supposed to be $\gamma_0 = 20 kN/m^3$, while the backfill, which has the same height as the extrados of the crown, has a weight per unit volume $\gamma_1 = 0.5\ \gamma_0$. The arch has been discretised in 100 voussoirs and the analysis has been carried out

by using a computer code set up on purpose. Two different deployments of the reinforcement have been considered: FRP at the extrados (type 1) and FRP at the intrados (type 2).

It is worth reminding that, in the considered arch, in absence of FRP, the minimum load factor is equal to 1.21; the collapse mechanism develops with hinges A and D at springing; hinge B forms at $z/L = 0.10 \div 0.25$ when z_L/L increases from 0.1 to 0.5, while hinge C ranges between $z/L = 0.50 \div 0.65$ (Clemente et al. 1995).

Let us consider the effect of FRP strengthening, with strips starting from the crown with increasing extension from 30% to 80% of the arch length. In Figs. 5 and 6 the load bearing capacity of the bridge, expressed by the load factor λ is plotted against z_L/L, for different values of the ratio between the FRP length (s_{FRP}) and the total length of the arch centre line (s_{ARCH}), in the two cases of extrados and intrados deployment.

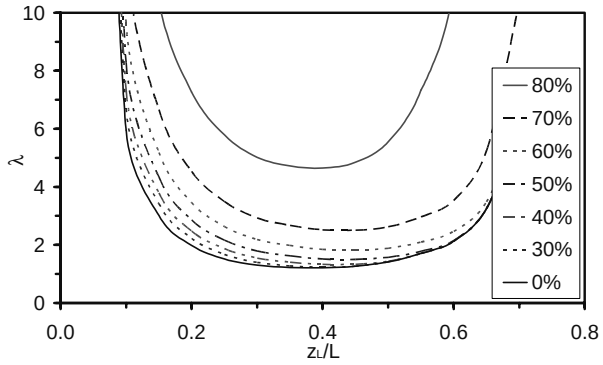

Figure 4 : Increase in load bearing capacity versus z_L/L for different ratios s_{FRP}/s_{ARCH} in the case of FRP at the extrados.

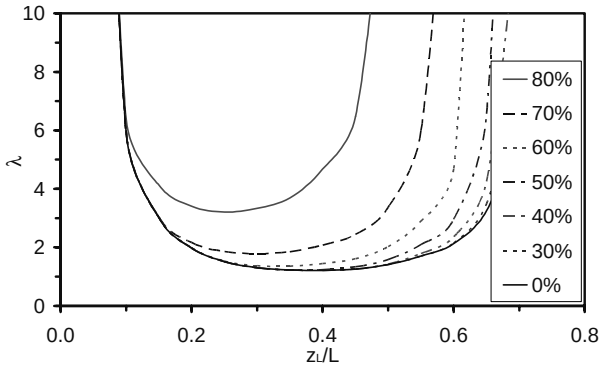

Figure 5 : Increase in load bearing capacity versus z_L/L for different ratios s_{FRP}/s_{ARCH} in the case of FRP at the intrados

In the case of FRP at the extrados, we note that, for small extension of FRP, an increase in load carrying capacity arises only for small ratios z_L/L (up to 0.5); for higher ratios, the influence of FRP is significant only for FRP extension grater than 60% of the arch.

In the case of FRP at the intrados, a significant increase in load carrying capacity arises for high values of z_L/L (> 0.5); for lower ratios, the contribution of FRP is low because the second hinge (B) forms close to the left springing.

In both cases, if the reinforcement is applied at the entire extrados or intrados no hinges mechanism is possible and the collapse will occur according to another limit state. Besides, the load condition relative to the minimum load factor changes with the FRP extension.

In Fig. 6, the minimum load factor is plotted against the FRP length, showing that FRP application succeed in increasing the load carrying capacity only for extensions $s_{FRP}/s_{ARCH} > 0.5$.

In order to check the local strength conditions, for a given extension s_{FRP}/s_{ARCH} of FRP, the shear force V, the compression force C and the FRP tension T are determined from the line of trust relative to the minimum load factor. In the present case, for FRP extension up to 80% of the arch length, it always result $V_d \le V_u$, provided the friction coefficient of masonry is not

lower than 0.5. The compression force C is plotted in Fig. 7 against the FRP extension; the resulting traction T in FRP can be used for the strip design, to ensure that $T < T_{tu}$ and $T < T_{bu}$.

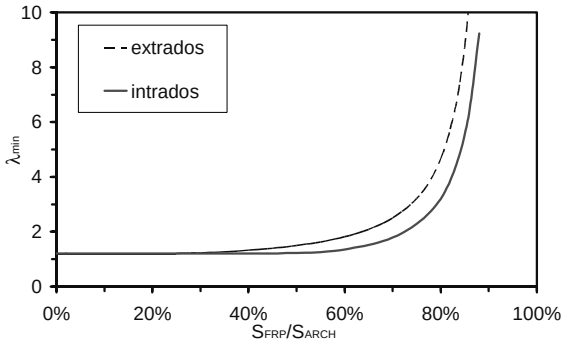

Figure 6 : Minimum load factor against s_{FRP}/s_{ARCH}

In the present case, a slight better performance of reinforcement deployment at the extrados results, by parity of FRP extension; however, it should be considered that the application of reinforcement at the intrados has the advantage to let the bridge remaining in service during the work. Clearly, architectural considerations deriving the visual impact of the reinforcement should also be taken into account, especially for historical bridges.

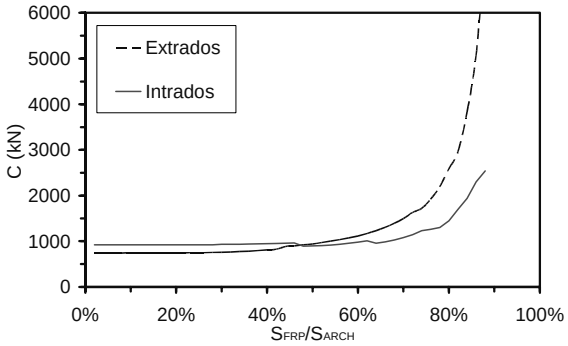

Figure 7 : Compression force against the values of FRP length

4.1 Multi-span arch bridges

For multi-span arch bridges, since the collapse may interest the piers (Brencich and De Francesco 2004), the load carrying capacity due to FRP strengthening may result lower than for single span bridges. Let us consider, for instance, the two-span arch bridge in Fig. 8, with the arches having the same geometrical characteristics as in the previous section. Both arches are supposed to be reinforced at the intrados with an extension $s_{FRP}/s_{ARCH} = 0.7$. The following loading condition is considered, in which the incoming travelling load q is uniformly distributed from the left springing of the left arch, to a generic section denoted by z_L of the right arch (Fig. 8).

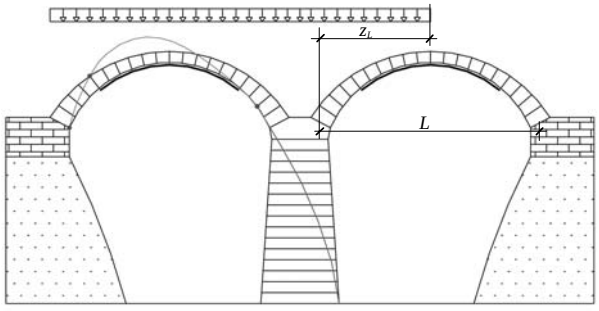

Figure 8 : The collapse of the pier

In Fig. 9 the load factor versus the end load abscissa z_L/L is plotted for both, single span and two-span arch bridges, having the same reinforcement extension. Only a slight difference arise in the present case; however, such a difference may become grater for multi-span bridges with high piers; in the latter case, the effectiveness of the reinforcement should be assessed by taking into account not only the arch but also the interaction with the piers.

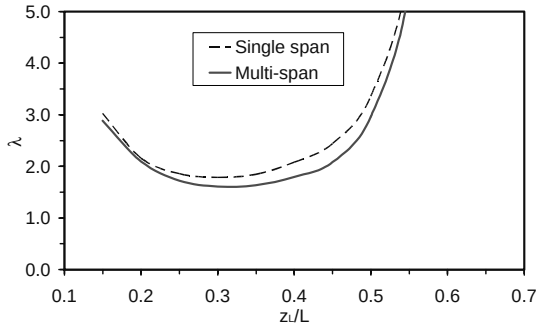

Figure 9 : Load factor λ versus z_L/L for single span and multi-span arch bridges.

5 CONCLUSIONS

In this paper the increase in load carrying capacity of arch bridges due to the application of FRP reinforcement, of variable length, at the intrados or at the extrados is analysed. According to the limit analysis kinematic approach, the limit load is obtained searching for the minimum in the subset of mechanisms allowed by the reinforcement. Beside, the conditions on local strength, to avoid failure of masonry in shear or in compression, and debonding or tensile failure of FRP are verified. Single span and two-span bridges under incoming travelling load have been considered and the effectiveness of a partial reinforcement has been pointed out.

A design procedure has been proposed, in which the extension of the reinforcement is designed under condition that the arch, when subjected to increasing travelling load, fails according to the hinges mechanism.

REFERENCES

Brencich A., De Francesco U. 2004. Assessment of multispan masonry arch bridges. Part I: a simplified approach. Part II: Examples and Applications", *Journal of Bridge Engineering, ASCE*, Vol. 9(6), p. 585-598.

Clemente P., Occhiuzzi A., Raithel A. 1995. Limit behavior of stone arch bridges, *Journal of Structural Engineering, ASCE*, Vol. 121(7), p. 1045-1050.

Faccio P., Foraboschi P., Siviero E. 2000. Collapse of masonry arch bridges strengthened using FRP laminates", *Proc. 3rd Int. Conference on ACMBS III, A.G. Razaqpur ed.*, Ottawa, p. 505-512.

Foraboschi, P. 2001. Strength assessment of masonry arch retrofitted using composite reinforcement, *Journal of British Masonry Society,* Vol. 15(1), p. 17-25.

Foraboschi, P. 2004. Strengthening of masonry arches with fiber-reinforced polymer strips, *Journal of Composites for Construction*, *ASCE,* Vol. 8(3), p. 191-202.

Heyman, J., 1966. The Stone Skeleton, *Int. J. of Solids and Structures*, Vol. 2, 249-279.

Heyman, J., 1969. The Safety of Masonry Arches, *Int. J. Mech. Sciences*, Vol. 11, 363-385.

Triantafillou T.C. 1998. Strengthening of masonry structures using epoxy-bonded FRP laminates, *Journal of Composites for Construction, ASCE*, Vol. 2(2), p.96-104.

Valluzzi, M.R., Valdemarca, M., Modena, C. 2001. Behaviour of brick masonry vaults strengthened by FRP laminates, *Journal of Composites for Construction, ASCE*, Vol. 5(3), p.163-169.